Electronic Structure of a Rigid Cyclic Diamide

Nicholas A. Besley,[†] Marie-Josèphe Brienne,[‡] and Jonathan D. Hirst*,[†]

School of Chemistry, University of Nottingham, University Park, Nottingham, NG7 2RD, U.K., and Chimie des Interactions moléculaires, UPR CNRS 285, Collège de France, 11 Place M. Berthelot, 75005 Paris, France

Received: July 7, 2000; In Final Form: October 13, 2000

Interest in the electronic structure of amides and polypeptides arises in part because optical spectroscopy such as electronic circular dichroism (CD) may be readily used to monitor conformational changes of peptides and proteins in solution. Our current, albeit somewhat incomplete, understanding of the relationship between polypeptide conformation and CD spectra has come in part from experimental and theoretical studies of model systems such as cyclic diamides. In this paper, we study the interactions between amide groups in a bridged cyclic diamide, diazabicyclo[2.2.2]octane-3,6-dione, through the measurement of its infrared (IR) and ultra-violet (UV) absorption and electronic CD spectra and through ab initio calculations of its electronic structure. The particular rigidity of the bridged cyclic diamide removes ambiguity regarding the conformation of the molecule in solution, which must remain close to the structure determined by X-ray crystallography. The theoretical study has been performed using the complete-active-space self-consistent-field and multi-configurational second-order perturbation theory methods. Solvent effects have been modeled using a self-consistent reaction field. The results of the electronic structure calculations agree well with the observed spectra and allow the origin of the bands to be assigned. The electronic spectrum is dominated by an intense $\pi_{nb}\pi^*$ transition, which is calculated to lie at 6.28 eV in the gas phase and 6.07 eV in solution. In addition, a number of less intense $n\pi^*$ and $\pi_{nb}\pi^*$ transitions are characterized. The results show that the electronic CD spectrum arises from $n\pi^*$ and $\pi_{nb}\pi^*$ transitions that can be considered to be localized on one amide group, while charge-transfer transitions do not make a significant contribution to the electronic CD spectrum.

Introduction

The amide group plays a key role in biopolymers, and consequently, its electric and optical properties are central to many important phenomena. For example, the electronic circular dichroism (CD) of proteins is a useful probe of secondary structure content and may be used to monitor protein folding.[1,2] For many years, the electronic structure of amides remained poorly understood. This has been partly because calculations on molecular electronic excited states are challenging,[3] and this turns out to be particularly true for amides. The recent advent of reliable excited-state methods and the necessary computational resources has prompted a flurry of theoretical studies of the electronic structure of amides.[4−13] These studies have led to a good understanding of the electronic structure of monoamides and have provided a foundation for calculations of protein CD.[14−16] However, the electronic structure of biopolymers is also dependent on the interaction between amide groups. The influence of these interactions on the spectroscopy of large biopolymers is not well understood. These systems are too large to study directly using theoretical techniques, and so, smaller model systems have to be examined. Recently, the gas-phase conformational energetics of substituted diketopiperazines have been studied in the context of understanding the formation of hydrogen-bonded tapes.[17,18] In this paper, we report our recent experimental and theoretical investigations of a bridged cyclic diamide. This provides an ideal system in which to study the interactions between amide groups.

Compared to monoamides, there have been relatively few studies of the electronic structure of diamides. The electronic absorption spectrum of the linear diamide *N*-acetyl-L-alanine-*N*′-methyl amide in aqueous solution was found to consist of a single intense, broad band centered at ∼6.6 eV, although only quite a narrow range of wavelength was measured.[19] This linear diamide has free rotation about the single bonds, and hence, an ensemble of conformations is populated in solution. Cyclic diamides have much less conformational freedom and are thus attractive model systems in which to study the interaction between two amide groups. The interactions between the two amide chromophores in cyclic diamides produce conformation-dependent effects on the CD spectra. For this reason and because of the simplicity of the structures, the CD spectra of cyclic diamides have been studied theoretically[20−25] and experimentally.[19,26−28] Perhaps the simplest cyclic diamide is **I**, diketopiperazine (DKP). There are experimental data on the

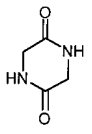

I

electronic absorption spectrum of DKP in gas phase,[29] solution,[29−31] and solid phase.[32] Significant twisting of the $\pi_{nb}\pi^*$ excited state of DKP has been observed using ultraviolet resonance Raman spectroscopy.[33]

Like the spectra of its linear counterpart, the spectra of DKP are dominated by the $\pi_{nb}\pi^*$ transition which appears as a broad

* Corresponding author. E-mail: jonathan.hirst@nottingham.ac.uk.
† University of Nottingham.
‡ Collège de France.

10.1021/jp0024524 CCC: $19.00
Published on Web 11/23/2000

band, with a maximum at 7.4 eV in the gas phase, 6.4 eV in aqueous solution, and 6.6 eV in the solid phase. The gas-phase data are believed to correspond to two species, the DKP monomer and the hydrogen-bonded dimer of DKP, with the 7.4 eV maximum in the gas-phase associated with the DKP dimer. The monomeric $\pi_{nb}\pi^*$ transition was assigned to the band at 6.4 eV.[29]

The most detailed information to date on the electronic structure of a diamide comes from complete-active-space self-consistent-field (CASSCF) and multi-configurational second-order perturbation theory (CASPT2) calculations of the valence and Rydberg states of planar DKP.[6] The two major features of the calculated electronic absorption spectrum are the $\pi_{nb}\pi^*$ transition at 6.0 eV (oscillator strength, $f = 0.58$) and the $\pi_b\pi^*$ transition at 8.7 eV ($f = 0.25$), in agreement with the experimental observation of a band at 6.4 eV ($f = 0.38 \pm 0.10$). A recent CASSCF/CASPT2 study[10] has investigated the electronic spectra of linear di- and tripeptides. A $\pi_{nb}\pi^*$ charge-transfer transition, in which charge is transferred from one amide group to the other, was found at $\sim$7.1−7.5 eV, in a region where there is an experimentally observed band in the electronic spectra of polypeptides. The calculations indicated that there is a significant relationship between the conformation of the diamide and the intensity of this transition. Although relatively small basis sets and active spaces were employed, the identification of a charge-transfer band of significant intensity is an important finding. However, the study of the conformational dependence of the electronic structure of the linear diamide is a little more speculative, due to the difficulty of making an appropriate comparison with experimental data. Recently,[34] the CD spectrum of *N*-(*N*-acetyl-L-alanyl)-L-alanine methylamide has been calculated using density functional theory. The relationship between the conformation and the CD spectrum was investigated, providing some qualitative insight. In another recent study,[35] the orientations of amide $\pi\pi^*$ transition moments in *N*-acetylglycinamide were determined from single-crystal preresonance Raman measurements. Comparison with the absorption and Raman spectra of *N*-methylacetamide and acetamide showed strong excitonic interactions.

Recently, in the context of the self-assembly of supramolecular complexes, a highly rigid cyclic diamide has been investigated.[36] Optically pure enantiomers of diazabicyclo[2.2.2]-octane-3,6-dione, **II**, have been synthesized, and their crystal structures have been solved.[36]

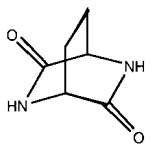

II

We have chosen **II** as a model in which to study the interactions between amide groups for a number of reasons. It is highly rigid, so there is little ambiguity regarding its conformation in solution. This is particularly important when using computationally expensive techniques, for which studying an ensemble of conformations is impractical. The molecule is chiral, so it may be characterized using CD spectroscopy, providing further information on its electronic structure. Fully ab initio calculations of chiroptical properties of molecules as large as **II** are relatively challenging, and there have been several methodological developments in this area.[37−39] Finally, we are interested in charge-transfer transitions, which by their nature cannot be studied through calculations on monoamides. Within a delocalized molecular orbital picture of **II** it is not possible to classify transitions rigorously as local or charge transfer. However, it is possible to determine the importance of the additional transitions arising in the diamide that have no analogue in monoamides. These transitions can be associated with the charge-transfer transitions observed in polypeptides of lower symmetry, such as a linear diamide.[10]

TABLE 1: Optimized Coordinates[a]

atom	*x* (Å)	*y* (Å)	*z* (Å)
C	1.211	−0.721	−0.520
C	0.028	1.253	0.202
C	−0.028	0.773	1.664
N	1.208	0.645	−0.419
O	2.068	−1.403	−1.076
H	1.855	1.183	−0.985
H	0.069	2.339	0.107
H	0.818	1.202	2.210
H	−0.948	1.141	2.131

[a] The other half of the molecule may be generated through symmetry.

In this study, we present the infrared (IR) and ultraviolet (UV) absorption and electronic CD spectra of **II** to explore interactions between amides in a well-defined model system. This establishes a reliable experimental reference point for the theoretical studies of diamides. We investigate the electronic structure of **II** theoretically, using CASSCF and CASPT2 calculations for the gas phase, and using CASSCF/SCRF and CASPT2-RF methods to model the influence of the solvent. The combination of experimental and theoretical data allows the interaction between amide groups to be described in detail.

Experimental Details

The CD spectra of the R,R-(−) enantiomer was measured from 200 to 300 nm using a Jobin Yvon Mark V spectrometer in three different solvents, water, methanol, and acetonitrile. A 0.2 cm path-length cell and 1×10^{-4} M solutions were used. IR spectra of the racemate were measured both in DMSO solution (at concentration of 1.1 g /100 g solution with a 0.1 mm cell in KBr) and in the solid phase (KBr pellet). UV spectra were measured in water at several concentrations: 1×10^{-4} M (0.2 cm path-length cell), 1×10^{-3} M (0.1 cm), and 5×10^{-3} M (0.02 cm).

Computational Details

The structure of **II** was optimized using Gaussian94.[40] Using the crystal structure as a starting point, we optimized the geometry of the *R,R* enantiomer of **II** in the gas phase at the second-order Møller−Plesset perturbation theory[41] level using the 6-31G* basis set within the C_2 point group. The optimized coordinates are included in Table 1. The amide ring lies approximately in the *x,y* plane, with the bridge carbons located in the positive *z* direction. The gas-phase vibrational spectrum was determined at the MP2 level with the 6-31G* basis and (with a reoptimized geometry) Becke's three-parameter hybrid DFT/HF method[42] using the Lee−Yang−Parr correlation functional (B3LYP) and the correlation-consistent valence double-ζ basis set (cc-pVDZ).[43] The DFT-optimized structure was highly similar to the MP2 structure. Both MP2 and B3LYP frequency calculations were performed because previous calculations on planar DKP had shown significant differences for the very lowest-frequency vibrations.

The gas-phase electronic structure was studied using the CASSCF/CASPT2 approach.[44,45] The CASSCF calculation

usually includes all states of interest, which are equally weighted. This is followed by CASPT2 calculations, which are performed for each root of the CASSCF wave function and account for dynamic correlation. This methodology has been used successfully to study monoamides[8] and DKP.[6] In this study, we are primarily concerned with valence-state properties, since Rydberg states will become less important in condensed phases. However, previous studies have shown that to compute the properties of valence states accurately, it is important to account for Rydberg states in order to reduce the mixing between Rydberg and valence states. This can be achieved by the appropriate choice of basis set combined with the removal of Rydberg orbitals.[8] These calculations are now discussed in more detail.

The atomic natural orbital (ANO) type[46] basis set was used with the following contractions: C, N, O 3s2p1d, and H 2s. This basis set does not contain functions that are suited to describing Rydberg states. Consequently, an additional set of 1s1p1d Rydberg-type functions was included. The Rydberg basis set derived to describe DKP[6] was used and placed at the center of mass of the amide ring.

To determine valence state properties, we used reference molecular orbitals in which the Rydberg orbitals have been removed. This reduces the Rydberg valence mixing. In principle, these reference orbitals can be determined in one large CASSCF calculation that includes all the important Rydberg orbitals in the active space. However, for the present system, this is too computationally expensive, and the Rydberg orbitals have to be removed in two steps. First, a CASSCF calculation was performed using an active space of five *a* and five *b* orbitals, denoted (5,5). These include the π_{nb} (π nonbonding) and n (oxygen lone-pair) orbitals of each symmetry, which are doubly occupied in the ground state. The remaining orbitals are the two π^* (π antibonding) orbitals and the 3s and 3p Rydberg orbitals. The SCF orbitals were used for reference, with the 1s and 2s orbitals of the heavy atoms kept frozen after the initial SCF calculation. An average state calculation was performed, equally weighted over eight *A* states. The 3s and 3p Rydberg orbitals were then removed and the resulting orbitals used for a subsequent calculation. The second step is similar to the first except that an active space of (6,5) was used. This includes the Rydberg 3d states. The Rydberg 3d orbitals were then removed, and the resulting set of orbitals are used for the computation of valence state properties.

The valence-state properties were determined in two calculations. The first included five *A* states, followed by one over four *B* states. A (4,4) active space was used. This includes the three π orbitals and the higher-energy n orbital for both symmetries. To reduce the problem of intruder states, we used a level shift[47] of 0.3 au in the CASPT2 calculations. Vertical excitation energies and transition moments were evaluated with reference to a single-root *A*-state calculation.

We turn now to the calculations in solvent. Even though **II** is relatively nonpolar, solvation may still have a significant effect on its electronic structure; for example, the Rydberg states will be destabilized by the solvent through Pauli repulsion. A realistic representation of the solvent requires many solvent molecules. In addition, the many possible solvent configurations must be considered. An effective, cheaper alternative is a continuum approach, in which the solute lies in a cavity surrounded by a continuous dielectric. While local solvent configuration can affect the CD of the solute,[48] accurate excited-state calculations of this type are not tractable for systems the size of **II** at the CASSCF/CASPT2 level of theory. A continuum description of the solvent has been implemented in the CASSCF with a self-consistent reaction field (SCRF) method.[49,50] In this approach, the reaction field is divided into electronic and nuclear components. The slow relaxation times of the nuclear degrees of freedom allow the nuclear component to be assumed to be constant during an electronic excitation. In contrast, the fast relaxation times of the electronic degrees of freedom require the nuclear components to be optimized for each electronic state in order to remain in equilibrium with the molecular charge distribution. For each root a CASPT2-RF[51] calculation is performed in which the SCRF field model is incorporated into CASPT2 by supplementing the one-electron Hamiltonian.

Calculations using a continuum model of the solvent require a cavity size to be chosen. In the present study, a spherical cavity of radius 8.2 a_o was used, based on van der Waals radii.[52] The continuous dielectric was characterized by a macroscopic dielectric constant $\epsilon = 80.0$ and a refractive index $\eta = 1.33$, corresponding to water. In this study, a repulsive potential that lies outside the cavity is included. This models the exchange repulsion of the solvent and maintains the solute charge distribution within the cavity. This potential has the effect of destabilizing the more diffuse Rydberg states and allows the valence states to be studied without the process of deletion of the Rydberg orbitals. Since there are no longer any Rydberg states in the lower-energy region of the electronic spectrum, it is no longer necessary to include the diffuse Rydberg functions in the basis set. This allows the size of the valence basis to be increased. ANO-type basis sets with the following contractions were used: C, N, O 4s3p1d, and H 2s. All calculations were performed using the MOLCAS4 program package.[53]

The chiral nature of **II** means that further details of its electronic structure may be gleaned from CD spectroscopy. CD is the differential absorption of left and right circularly polarized light. The intensity of a band in the CD spectrum is given by the rotatory strength, *R*. The rotatory strength of an electronic transition from the ground state (Ψ_0) to an excited state (Ψ_f) can be expressed in the origin-independent velocity form as[54]

$$R^{v} = \frac{e^2}{2m_e^2\omega_{f0}}\rho_{0f}\cdot L_{f0} \qquad (1)$$

where $\omega_{f0} = 2\pi(E_f - E_0)/h$, ρ is the momentum, and L the angular momentum. In the length form, R is origin-dependent and can be expressed as[54]

$$R^{r} = \frac{ie}{2m_e}\mu_{0f}\cdot L_{f0} \qquad (2)$$

in which μ is the electronic dipole moment. In general, for approximate wave functions, the two forms do not agree. Using the CAS state interaction method,[55] we computed appropriate transition moments and evaluated the CD spectrum.

Results

The UV spectrum in water of **II** at a concentration of 0.0001 M (Figure 1) shows a band at 6.42 eV (193 nm) with a maximum intensity of 12 000 M^{-1} cm^{-1}. From the spectrum, we estimate the oscillator strength of this transition to be 0.61. In addition to this band, there is a band at 5.51 eV (225 nm) with an oscillator strength of ~0.12. Changing the concentration has little effect on the intensity of the bands at 6.42 and 5.51 eV, suggesting that these bands correspond to electronic transitions associated with monomeric units. However, at lower concentration, there is a loss in intensity at 5.85 eV (212 nm).

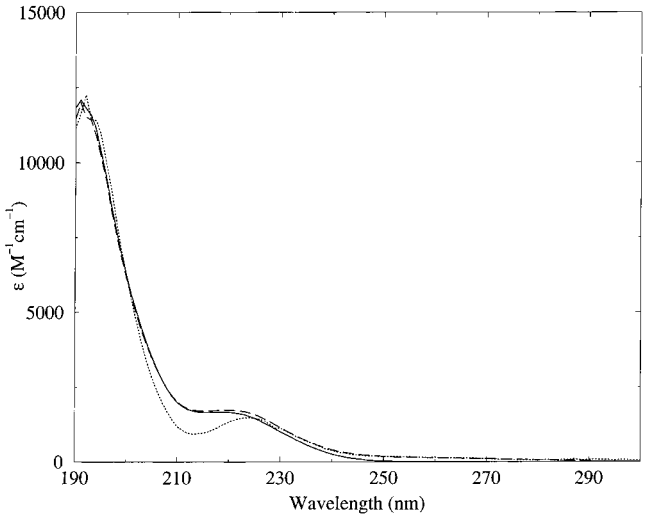

Figure 1. UV absorption spectra of **II** in water at 5×10^{-3} M (solid line), 1×10^{-3} M (dashed line), and 1×10^{-4} M (dotted line).

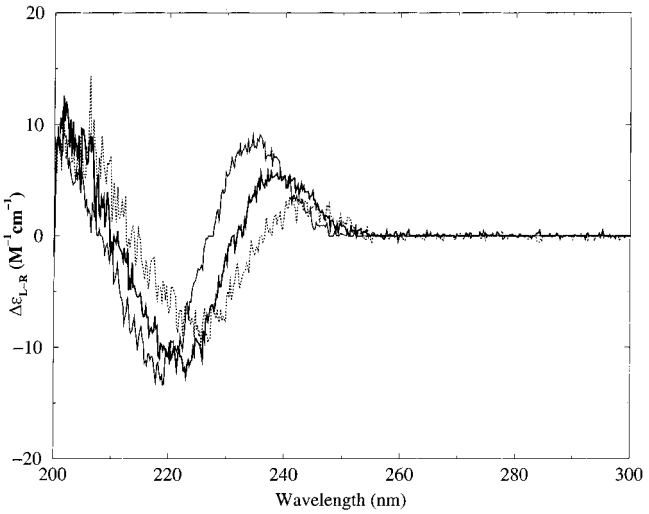

Figure 2. CD spectra of **II** in water (solid line), methanol (bold line), and acetonitrile (dotted line).

The spectrum also shows no evidence of transitions to Rydberg states. This is also observed in the condensed-phase UV spectra of monoamides.[56] Figure 2 shows the CD spectra measured in three solvents, water, methanol and acetonitrile. All spectra have a three-band pattern. In water, these bands lie at 5.30 eV (234 nm), 5.69 eV (218 nm), and 6.23 eV (199 nm), with rotational strengths of $+0.10 \times 10^{-40}$, -16×10^{-40}, and $+10 \times 10^{-40}$ cgs, respectively. Rotatory strengths were estimated from the spectra on the basis of the area of the peaks computed from the bandwidths and maxima, assuming Gaussian-shaped bands. Strongly overlapping bands may confound such estimates, but our calculations would provide some indication of such a problem. In less polar solvents, the spectra are shifted to higher wavelengths. The relative intensities of the bands also change. In particular, the intensity of the low-energy band decreases. The experimental CD data are summarized in Table 2.

Figure 3 shows the IR spectra of (−)-**II** measured in DMSO solution and in solid state. In both spectra, the amide I band is prominent and lies at about 1700 cm^{-1}. This band corresponds to the C−O stretch. The N−H stretch band appears at about 3200 cm^{-1}. Table 3 shows the calculated IR spectrum computed using MP2 and DFT. The MP2- and DFT-optimized ground-state energies were computed to be −491.958 and −493.458 au, respectively. Only vibrations with significant calculated intensities are shown. Both calculations qualitatively predict the shape of the spectrum. The N−H stretch is computed to lie at around 3600−3640 cm^{-1}, which is higher than that in the experiment. The splitting of this band is small (∼1 cm^{-1}). The calculations predict the C−O stretch (amide I band) to lie at 1820−1830 cm^{-1}. The splitting of this band is also small, at most 3 cm^{-1}, as predicted by the MP2 calculation. The relative intensities of these two bands are ∼600 and ∼100 km mol^{-1}. In DKP,[6] one band is very weak: the corresponding intensities are ∼700 and ∼0 km mol^{-1}. In **II**, the amide II band at around 1450 cm^{-1} splits by about 20 cm^{-1}, but all the intensity appears in one component.

The calculated electronic spectra and experimental data are presented in Table 4. In the gas phase, the spectrum is dominated by a broad $2^1B(\pi_{nb}\pi^*)$ transition. The transition energy and oscillator strength, *f*, for this transition are 6.61 eV and 0.63, respectively, in good agreement with the experimental data. The oscillator strength of 0.63 is approximately double the oscillator strengths observed for monomeric amide $\pi_{nb}\pi^*$ transitions. This suggests that this band corresponds to one of the two bands arising from the exciton splitting of the monomer $\pi_{nb}\pi^*$ transitions. Consequently, we can regard this transition as corresponding to a local $\pi_{nb}\pi^*$ transition. Within the C_2 point group, one of these bands has *A* symmetry and one *B* symmetry. Thus, the 2^1B and 3^1A transitions form a coupled pair. This gives a splitting of 0.33 eV. These assignments agree with those for the linear diamide,[10] where the valence $\pi_{nb}\pi^*$ transitions were found to lie between 6.1 and 6.7 eV, with splittings of between ∼0 and 0.5 eV. In the linear diamide, the oscillator strength of these two bands are generally comparable at ∼0.3. This contrasts with cyclic diamides, such as DKP and **II**, where the relative orientation of the monoamide $\pi_{nb}\pi^*$ transition moments lead to one very intense band and one very weak band. Monomeric $n\pi^*$ transitions typically lie at ∼5.5 eV. The corresponding $n\pi^*$ transitions in **II** are weak and appear at 5.47 and 5.48 eV.

The transitions described above can be associated with transitions occurring in monoamides. In diamides, however, there is an additional set of transitions. In molecules of lower symmetry, these are charge-transfer transitions, characterized by the movement of charge from one amide group to another. **II** belongs to the C_2 point group. In a delocalized molecular orbital picture of **II**, it is not possible to characterize these transitions rigorously as charge-transfer transitions. However, by considering small distortions of **II**, we can regard these transitions as corresponding to charge-transfer transitions. The two $\pi_{nb}\pi^*$ charge-transfer transitions are computed to lie at 7.51 and 7.56 eV. One of these bands, (3^1B) has a significant oscillator strength of 0.05. Although this band is not as intense

TABLE 2. Experimental CD Data

	water		methanol		acetonitrile	
solvent	Δ*E* (eV) (nm)	*R* (10^{-40} cgs)	Δ*E* (eV) (nm)	*R* (10^{-40} cgs)	Δ*E* (eV) (nm)	*R* (10^{-40} cgs)
band 1	5.30 (234)	+10	5.21 (238)	+6	5.12 (242)	+4
band 2	5.69 (218)	−16	5.58 (222)	−17	5.48 (226)	−12
band 3	6.23 (199)	+10	6.11 (203)	+10	6.08 (204)	+11

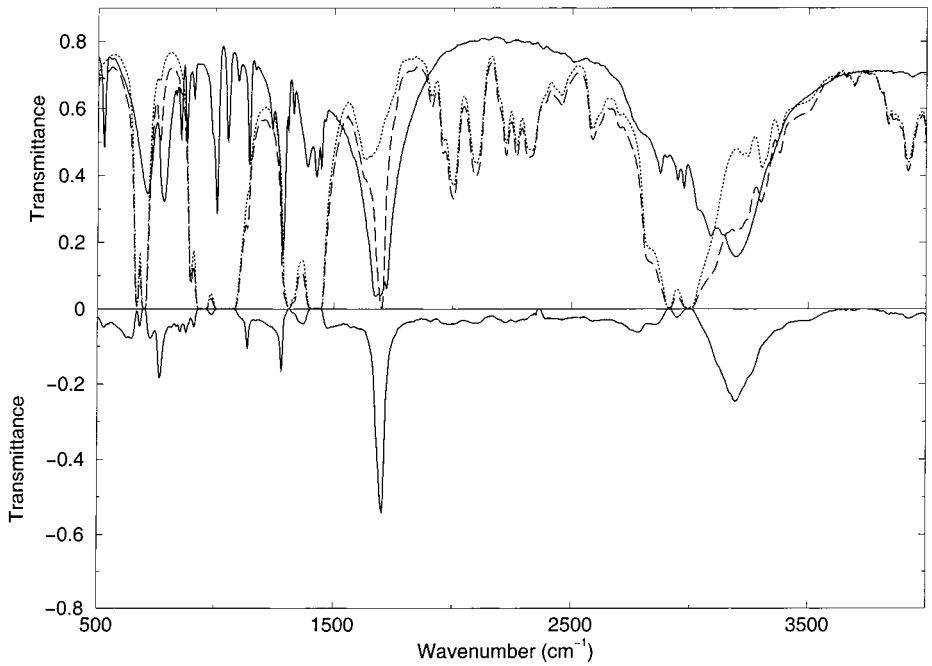

Figure 3. IR spectra. Top panel: solid **II** (solid line), 1.1 g % **II** in DMSO solution (dashed line), and pure DMSO (dotted line). Lower panel: 1.1 g% **II** in DMSO minus DMSO.

TABLE 3: Calculated Vibrational Spectrum

MP2/6-31G*		B3LYP/(cc-pVDZ)		
frequency (cm^{-1})	I ($kmmol^{-1}$)	frequency (cm^{-1})	I ($kmmol^{-1}$)	assignment[a]
391	24	392	23	oop bend of amide H atoms
416	133	413	112	oop bend of amide H atoms
420	63	420	39	oop bend of all H atoms + O atoms
557	25	553	16	oop bend of amide + bridge H atoms
947	16	920	16	wag of CH + alternate CH_2H atoms
1033	17	1014	19	N−C(CH) motion
1087	21	1047	23	oop bend of CH H atoms; ip bend of amide H atoms
1183	28	1142	29	wag of CH and CH_2H atoms
1347	60	1292	64	wag of CH and alternate CH_2H atoms
1406	0	1367	18	wag of all H atoms; ip bend of amide H atoms
1455	107	1422	78	C(O)-N stretch (amide II band)
1827	122	1819	682	C−O stretch (amide I band)
1830	580	1819	147	C−O stretch (amide I band)
3119	14	3052	21	CH_2 stretch
3127	20	3063	29	CH_2 stretch
3188	19	3114	29	CH_2 stretch
3192	11	3144	19	C(CH)-H stretch
3641	95	3605	64	N−H stretch
3642	25	3606	16	N−H stretch

[a] Abbreviations: oop, out of plane; ip, in plane.

TABLE 4: Calculated Electronic Spectrum and Experimental Data

	gas phase			solution			experiment CD/UV (water)	
state	ΔE (eV)	f	μ (D)	ΔE (eV)	f	μ (D)	ΔE (eV)	f
1^1A(g.s.)			3.16			3.34		
$2^1A(n\pi^*)$	5.48	0.003	2.05	5.70	0.003	1.75	5.30	<0.05
$3^1A(\pi\pi^*)$	6.28	0.027	3.52	6.07	0.042	3.81	5.69	<0.05
$4^1A(\pi\pi^*)$	7.56	0	2.44	7.22	0	2.69		
$5^1A(n\pi^*)$	8.43	0.016	1.90	8.05	0.009	1.43		
$1^1B(n\pi^*)$	5.47	0.005	1.98	5.77	0.004	1.73		
$2^1B(\pi\pi^*)$	6.61	0.630	3.26	6.48	0.628	3.27	6.23−6.42	0.608
$3^1B(\pi\pi^*)$	7.51	0.046	3.07	7.10	0.027	3.30		
$4^1B(n\pi^*)$	8.04	0.055	2.60	7.68	0.043	2.60		

as some of the charge-transfer bands obtained for linear diamides,[10] it confirms that bands observed in the spectra of polypeptides in this region are likely to arise from charge-transfer transitions. A larger splitting (0.39 eV) is found for the charge-transfer $n\pi^*$ bands, which are computed to lie at 8.04 and 8.43 eV.

The inclusion of solvent in the calculations has a modest effect on the valence states (although it has considerable effect

TABLE 5: Rotatory Strengths

	gas phase			solution			exp. (water)	
state	ΔE (eV)	R^v (10^{-40} cgs)	R^r (10^{-40} cgs)	ΔE (eV)	R^v (10^{-40} cgs)	R^r (10^{-40} cgs)	ΔE (eV)	R^{exp} (10^{-40} cgs)
2^1A	5.48	−3.6	−4.8	5.70	−2.7	−4.3		
3^1A	6.28	−28.5	−22.9	6.07	−25.1	−21.5	5.69	−16
4^1A	7.56	−0.1	−0.2	7.22	+0.2	0		
5^1A	8.43	−1.1	−0.9	8.05	0	0		
1^1B	5.47	+11.9	+9.2	5.77	+9.1	+9.1	5.30	+10
2^1B	6.61	+27.0	+21.7	6.48	+27.1	+25.1	6.23	+10
3^1B	7.51	+2.1	+1.8	7.10	+1.2	+1.3		
4^1B	8.04	+4.9	+4.2	7.68	+3.5	+2.5		

on the Rydberg states). All the $\pi_{nb}\pi^*$ bands undergo a red shift of between 0.1 and 0.35 eV. The resulting transition energy of the intense $\pi_{nb}\pi^*$ band of 6.48 eV is in agreement with the experiment. The lower-energy $1^1B(n\pi^*)$ and $2^1A(n\pi^*)$ transitions are blue-shifted and are calculated to lie at about 5.7 eV. This type of blue shift is typical for amides in water.[32] These calculated values lie about 0.3−0.4 eV above the experimental values, which were assigned on the basis of the CD spectra (see later). It is probable that some of this error may be attributed to the size of the basis set. Calculations using a smaller basis set (not shown) give larger transition energies that are further from the experimental values. This indicates that a more complete basis may result in increasingly accurate calculated energies. Presently, the size of the system precludes an increase in the basis set beyond that reported in this study.

The computed rotatory strengths (Table 5) show that only four transitions make a significant contribution to the CD in the 190−260 nm region. Initially we shall discuss the results in solution. The $2^1B(\pi_{nb}\pi^*)$ transition results in an intense positive band, calculated to lie at 6.48 eV. The $3^1A(\pi_{nb}\pi^*)$ transition leads to an intense negative band at 6.07 eV, despite having a relatively weak electronic transition moment. The remaining two bands, arising from the $2^1A(n\pi^*)$ and $1^1B(n\pi^*)$ transitions, are of opposite signs. Due to the small splitting of the $n\pi^*$ transitions, only one positive band results and is predicted to lie at 5.7 eV. These bands combine to reproduce the three-band pattern of the experimental spectra, albeit shifted slightly to a higher energy. The four bands that have significant intensity in the CD spectrum arise from electronic transitions that can be regarded as local in origin. The rotatory strengths arising from electronic transitions that can be associated with charge-transfer transitions are low. The calculations tend to overestimate the rotatory strengths of the $\pi_{nb}\pi^*$ bands. The neglect of the local structure of the solvent may introduce some error into the calculated rotatory strengths. However, the qualitative shape of the experimental spectrum is reproduced. In water, the intensity of the low-energy band is overestimated. The calculated intensities for this band agree better with the CD spectrum measured in acetonitrile. In this spectrum, the intensity of this band is considerably lower. This indicates that the intensity of this band is sensitive to hydrogen bonding. The solvation model used in our calculations will not describe hydrogen bonds and would be expected to provide a better model for a non-hydrogen-bonding solvent.

The calculated spectrum in the gas phase has the same general shape as that in solution. There are some small differences in the calculated band intensities. In particular, the band arising from the 3^1A transition is more intense than that for the 2^1B transition. Both velocity and length formalisms are in good agreement, indicating that the quality of the wave function is good.

Discussion

It is unlikely that electronic structure calculations of biopolymers of more than a few monomer units will be possible soon. Consequently, it is necessary to study well-defined model systems in order to establish general features and principles which can be integrated into studies of larger systems. Cyclic diamides are the simplest systems in which to study interactions between amide groups. Furthermore, the rigidity of bridged cyclic diamide **II** removes ambiguity regarding its structure in solution.

The UV absorption spectrum is typical of amides, with an intense $\pi_{nb}\pi^*$ band having a shoulder on the low-energy side. The peak of this intense band lies at 6.48 eV in the gas phase, which is typical of secondary and tertiary amides. In addition, there are also a number of weak local and charge-transfer transitions. The CD spectrum has more features and provides a more detailed probe of the electronic structure. The good agreement between the calculated and experimental CD spectra allows the bands in the experimental spectra be assigned to electronic transitions. The three bands comprise four electronic transitions, arising from $n\pi^*$ and $\pi_{nb}\pi^*$ transitions which are local in origin. The energy separation of local $\pi_{nb}\pi^*$ transitions is sufficient to result in two distinct bands, one positive and one negative. The energy separation between the local $n\pi^*$ bands is small. Consequently, only one band results, despite the differing sign of the two bands. Presently, calculations of the CD spectra of proteins based on monoamide units do not include charge-transfer transitions.[14−16] The role of charge-transfer transitions in the CD of proteins is currently not well understood. The results of this study show that in **II** charge-transfer transitions do not make a significant contribution to the CD spectrum. This provides some evidence that charge-transfer bands may not be important in protein CD. However, it is likely that the intensity of these bands will be sensitive to conformation.

Vibrational spectroscopy is also used extensively to probe the conformation of polypeptides and proteins.[57] Again, ab initio calculations of IR spectra of proteins are infeasible, and more approximate methods must be employed. Force fields for smaller systems are developed and used as models for the vibrations in larger polypeptides. One such example is DKP,[58] which can serve as a model for vibrations of the cis peptide group. This type of approach depends on the transferability of force constants between different structures, and the optimum parameters are those which maximize transferability. The addition of a bridge to DKP provides an opportunity to study the effect of a small structural change on vibrational spectra. The most notable difference is on the amide I band (C−O stretch), which lies at about 1700 cm^{-1} in the experimental spectrum. The splitting of this band is calculated to be significantly less than that in DKP, and both bands have significant intensity. The N−H stretch is computed to lie approximately 20 cm^{-1} higher than that in DKP, but for both systems, the splitting is predicted to be small.

Conclusions

In this study, a bridged cyclic diamide has been investigated in detail by both experimental and theoretical techniques. This system is attractive because it enables the interaction between amide groups to be investigated while its rigid structure removes ambiguity regarding its structure in solution. The UV spectrum is dominated by a single broad band, while the CD spectrum has a three-band pattern. The theoretical studies provide insight into the experimental data, the most important result being the identification of charge-transfer bands. In particular, these transitions do not make a significant contribution to the CD spectrum. While this does not preclude them from being important in protein CD, it provides some support for techniques such as the matrix method[59,60] which predict the CD spectrum of proteins on the basis of monomer units. The CD calculations presented in this study are some of the highest-level CD calculations on molecules the size of **II**.

The scope for extending studies on **II** are limited, although one approach would be to decorate the structure with additional groups and characterize the new interactions. More approximate theoretical methods are required to study larger systems. The quality of such approximations should be assessed on **II**, where there is the complexity of interacting amide groups without conformational flexibility obscuring comparisons between experiment and theory. Thus, our extensive characterization of **II** will hopefully prove to be a useful stepping stone on the way to greater insight into the electronic structure of proteins.

Acknowledgment. M.J.B thanks Miss Florence Robinet and Dr. Jeanine Milhaud (Phisicochimie biomoléculaire et cellulaire, Paris 6) for their assistance in measuring CD spectra. Financial support from the National Science Foundation and the Engineering and Physical Sciences Research Council is gratefully acknowledged. Acknowledgment is made to the donors of the Petroleum Research Fund, administered by the ACS, for partial support of this work.

References and Notes

(1) Fasman, G. D. *Circular Dichroism and the Conformational Analysis of Biomolecules*; Plenum Press: New York, 1996.
(2) Nakanishi, K.; Berova, N.; Woody, R. W. *Circular Dichroism Principles and Applications*; VCH: New York, 1994.
(3) Bartlett, R. J.; Stanton, J. F. *Rev. Comput. Chem.* **1994**, *5*, 65−169.
(4) Hirst, J. D.; Hirst, D. M.; Brooks, C. L., III. *J. Phys. Chem.* **1996**, *100*, 13487−13491.
(5) Hirst, J. D.; Hirst, D. M.; Brooks, C. L., III. *J. Phys. Chem. A* **1997**, *101*, 4821−4827.
(6) Hirst, J. D.; Persson, B. J. *J. Phys. Chem. A* **1998**, *102*, 7519−7524.
(7) Besley, N. A.; Hirst, J. D. *J. Phys. Chem. A* **1998**, *102*, 10791−10797.
(8) Serrano-Andrés, L.; Fülscher, M. P. *J. Am. Chem. Soc.* **1996**, *118*, 12190−12199.
(9) Serrano-Andrés, L.; Fülscher, M. P. *J. Am. Chem. Soc.* **1996**, *118*, 12200−12206.
(10) Serrano-Andrés, L.; Fülscher, M. P. *J. Am. Chem. Soc.* **1998**, *120*, 10912−10920.
(11) Szalay, P. G.; Fogarasi, G. *Chem. Phys. Lett.* **1997**, *270*, 406−412.
(12) Tozer, D. J.; Amos, R. D.; Handy, N. C.; Roos, B. O.; Serrano-Andrés, L. *Mol. Phys.* **1999**, *97*, 859−868.
(13) Besley, N. A.; Hirst, J. D. *J. Am. Chem. Soc.* **1999**, *121*, 8559−8566.
(14) Besley, N. A.; Hirst, J. D. *J. Am. Chem. Soc.* **1999**, *121*, 9636−9644.
(15) Hirst, J. D.; Besley, N. A. *J. Chem. Phys.* **1999**, *111*, 2846−2847.
(16) Woody, R. W.; Sreerama, N. *J. Chem. Phys.* **1999**, *111*, 2844−2845.
(17) Palacin, S.; Chin, D. N.; Simanek, E. E.; MacDonald, J. C.; Whitesides, G. M.; McBride, M. T.; Palmore, G. T. R. *J. Am. Chem. Soc.* **1997**, *119*, 9, 11807−11816.
(18) McDonald, J. C.; Whitesides, G. M. *Chem. Rev.* **1994**, *94*, 2383−2420.
(19) Bowman, R. L.; Kellerman, M.; Johnson, W. C. *Biopolymers* **1983**, *22*, 1045−1070.
(20) Fleischhauer, J.; Grötzinger, J.; Kramer, B.; Krüger, P.; Wollmer, A.; Woody, R. W.; Zobel, E. *Biophys. Chem.* **1994**, *49*, 141−152.
(21) Hooker, T. M.; Bayley, P. M.; Radding, W.; Schellman, J. A. *Biopolymers* **1974**, *13*, 549−566.
(22) Richardson, F. S.; Pitts, W. *Biopolymers* **1974**, *13*, 703−724.
(23) Sathyanarayana, B. K.; Applequist, J. *Int. J. Peptide Res.* **1985**, *26*, 518−527.
(24) Snow, J. W.; Hooker, T. M. *J. Am. Chem. Soc.* **1975**, *97*, 3506−3511.
(25) Snow, J. W.; Hooker, T. M.; Schellman, J. A. *Biopolymers* **1977**, *16*, 121−142.
(26) Pancoska, P.; Fric, I.; Blaha, K. *Collect. Czech. Chem. Commun.* **1979**, *44*, 1296−1311.
(27) Madison, V.; Young, P. E.; Blout, E. R. *J. Am. Chem. Soc.* **1976**, *98*, 5358−5364.
(28) Strickland, E. H.; Wilchek, M.; Horwitz, J.; Billups, C. *J. Biol. Chem.* **1970**, *245*, 4168−4177.
(29) Kaya, K.; Nagakura, S. *Theor. Chim. Acta* **1967**, *7*, 124−132.
(30) Ham, J. S.; Platt, J. R. *J. Chem. Phys.* **1952**, *20*, 335−336.
(31) Nielsen, E. B.; Schellman, J. A. *J. Phys. Chem.* **1967**, *71*, 2297−2304.
(32) Kaya, K.; Nagakura, S. *J. Mol. Spectrosc.* **1972**, *44*, 279−285.
(33) Song, S.; Asher, S. A.; Krimm, S.; Shaw, K. D. *J. Am. Chem. Soc.* **1991**, *113*, 1155−1163.
(34) Bour, P. *J. Phys. Chem. A.* **1999**, *103*, 5099−5104.
(35) Pajcini, V.; Asher, S. A. *J. Am. Chem. Soc.* **1999**, *121*, 10942−10954.
(36) Brienne, M.-J.; Gabard, J.; Leclercq, M.; Lehn, J.-M.; Cesario, M.; Pascard, C.; Chevé, M.; Dutruc-Rosset, G. *Tetrahedron Lett.* **1994**, *35*, 8157−8160.
(37) Pulm, F.; Schramm, J.; Grimme, S.; Peyerimhoff, S. D. *Chem. Phys.* **1997**, *224*, 143−155.
(38) Kondru, R. K.; Wipf, P.; Beratan, D. N. *Science* **1998**, *282*, 2247−2250.
(39) Pedersen, T. B.; Koch, H.; Ruud, K. *J. Chem. Phys.* **1999**, *110*, 2883−2892.
(40) Frisch, M. J.; Trucks, G. W.; Schlegel, H. B.; Gill, P. M. W.; Johnson, B. G.; Robb, M. A.; Cheeseman, J. R.; Keith, T. A.; Petersson, G. A.; Montgomery, J. A.; Raghavachari, K.; Al-Laham, M. A.; Zakrzewski, V. G.; Ortiz, J. V.; Foresman, J. B.; Cioslowski, J.; Stefanov, B. B.; Nanayakkara, A.; Challacombe, M.; Peng, C. Y.; Ayala, P. Y.; Chen, W.; Wong, M. W.; Andres, J. L.; Replogle, E. S.; Gomperts, R.; Martin, R. L.; Fox, D. J.; Binkley, J. S.; Defrees, D. J.; Baker, J.; Stewart, J. P.; Head-Gordon, M.; Gonzalez, C.; Pople, J. A. *Gaussian 94*, Revision A.1; Gaussian, Inc.: Pittsburgh, PA, 1995.
(41) Moller, C.; Plesset, M. S. *Phys. Rev.* **1934**, *46*, 618−622.
(42) Becke, A. D. *J. Chem. Phys.* **1993**, *98*, 5648.
(43) Dunning, T. H. *J. Chem. Phys.* **1989**, *90*, 1007−1023.
(44) Roos, B. O. *Adv. Chem. Phys.* **1987**, *69*, 399−446.
(45) Andersson, K.; Malmqvist, P.-Å; Roos, B. O. *J. Chem. Phys.* **1992**, *96*, 128−1226.
(46) Widmark, P.-O.; Malmqvist, P.-Å; Roos, B. O. *Theor. Chim. Acta* **1990**, *77*, 291−306.
(47) Roos, B.; Andersson, K. *Chem. Phys. Lett.* **1995**, *245*, 215−223.
(48) Fidler, J.; Rodger, A.; Rodger, P. M. *J. Am. Chem. Soc.* **1994**, *116*, 7266−7273.
(49) Karlström, G. *J. Phys. Chem.* **1988**, *92*, 1315−1318.
(50) Karlström, G. *J. Phys. Chem.* **1989**, *93*, 4952−4955.
(51) Serrano-Andrés, L.; Fülscher, M. P.; Karlström, G. *Int. J. Quantum Chem.* **1997**, *65*, 167−181.
(52) Bondi, A. *J. Phys. Chem.* **1964**, *68*, 441−451.
(53) Andersson, K.; Blomberg, M. R. A.; Fülscher, M. P.; Karlström, G.; Lindh, R.; Malmqvist, P.-Å; Neogrády, P.; Olsen, J.; Roos, B. O.; Sadlej, A. J.; Schütz, M.; Seijo, L.; Serrano-Andrés, L.; Siegbahn, P. E. M.; Widmark, P.-O. *MOLCAS*, Version 4; Lund University: Lund, Sweden, 1997.
(54) Pedersen, T. B.; Hansen, A. E. *Chem. Phys. Lett.* **1995**, *246*, 1−8.
(55) Malmqvist, P.-Å; Roos, B. O. *Chem. Phys. Lett.* **1989**, *155*, 189−194.
(56) Basch, H.; Robin, M. B.; Kuebler, N. A. *J. Chem. Phys.* **1968**, *49*, 5007−5018.
(57) Krimm, S.; Bandekar, J. *Adv. Protein Chem.* **1986**, *38*, 181−367.
(58) Cheam, T. C.; Krimm, S. *Spectrochim. Acta., Part A* **1984**. *40*, 503−517.
(59) Woody, R. W. *J. Chem. Phys.* **1968**, *49*, 4797−4806.
(60) Bayley, P. M. *Prog. Biophys. Mol. Biol.* **1973**, *27*, 3−76.